2022

Oil Circulation Rate Measurements with Flow-through and Evacuated Type Sampling Cylinders

Syed Angkan Haider

Xin Wang

Stefan Elbel

Oil Circulation Rate Measurements with Flow-through and Evacuated Type Sampling Cylinders

Syed Angkan HAIDER[1], Xin WANG[1], Stefan ELBEL[1,2]*

[1]Air Conditioning and Refrigeration Center, Department of Mechanical Science and Engineering, University of Illinois at Urbana-Champaign, 1206 West Green Street, Urbana, IL 61801, USA

[2]Creative Thermal Solutions, Inc., 2209 North Willow Road, Urbana, IL 61802, USA

* Corresponding Author: elbel@illinois.edu

ABSTRACT

To reduce the frictional wear and tear between the moving parts of the compressor, most vapor compression systems make use of different lubricating oils. The oil can leave the compressor and can get circulated around the system or get retained at specific locations. Oil circulation rate (OCR) is defined as the percentage by mass of circulating oil in the oil-refrigerant mixture. Since OCR is known to affect system performance, it is very important to be able to accurately measure OCR. The ASHRAE standard 41.4 describes the method of OCR measurement employing an oil sampling technique with an evacuated type sampling cylinder. However, this method has certain limitations, and past research on the topic has shown that results can vary between evacuated type and flow-through type sampling cylinders.

The present work provides an experimental comparison between sampling results for the flow-through type and evacuated type sampling cylinders in a vapor compression system using R134a as refrigerant and PAG 46 oil as lubricant. The compressor speed was varied from 1500 min^{-1} to 2500 min^{-1}. The OCR sampling data were recorded with the system at steady-state, and online oil concentration sensor data were also taken to provide additional insights. Details of the flow patterns in the evacuated sampling cylinder were observed using a high-speed camera, and some of the key factors affecting OCR data obtained using the evacuated sampling cylinder were discussed.

1. INTRODUCTION

The primary purpose of using oil in vapor compression systems is to lubricate the moving parts of the compressor and to minimize wear and tear due to friction. This, in turn, helps to make sure that the longevity of the compressor is extended. The oil also helps to dissipate heat, and to reduce noise and vibrations. Inside the compressor, the lubricating oil also acts as a sealant and helps to maintain good volumetric efficiency. Despite being mostly advantageous, lubricating oil in vapor compression systems has some disadvantages too. While the oil is usually required to stay within the compressor only, the oil, mixed with refrigerant, can leave the compressor and either be in circulation or get retained in heat exchangers, receivers, and accumulators. The presence of oil in the system also affects flow regimes and may negatively impact refrigerant distribution. The properties of pure refrigerant within the system are altered. From the works of Radermacher *et al.* (2006), Youbi-Idrissi and Bonjour (2008) and several others, it was found that with high OCR, the amount of oil retained in the evaporator increases thus decreasing the heat transfer area and reducing the heat transfer coefficient. Shen and Groll (2005) found that most studies report that oil presence increases pressure drop during evaporation and condensation. At the system level, the works of Liu and Hrnjak (2016) show that with the increase of OCR, both system capacity and COP drop.

The presence of excessive oil can have detrimental effects on the performance at both the system level and the component level. Considering this, nowadays, there is an industry trend towards low-OCR compressors, and with the OCR values getting smaller and smaller, it has become very important to be able to measure OCR accurately. There are a variety of in-situ methods of OCR measurement which depend on different physical fluid properties such as density, speed of sound, refractive index, etc. Xu and Hrnjak (2017) demonstrated a novel method to measure OCR using a high-speed camera and video processing techniques. Their method relied on measurements of oil film thickness, oil film average velocity, oil droplet size, oil droplet velocity, and system mass flow rate.

All these methods require calibration, and this is contingent upon the specifics of the test, and the oil-refrigerant combinations used. The calibration is done against the OCR sampling technique described by the ASHRAE standard 41.4 (2015) which employs an evacuated type sampling cylinder with a dead end, performed at the liquid line. But this method might be prone to some limitations, e.g., immiscible combinations of oil and refrigerant, orientation of the sampling cylinder, valve opening speed, vacuum time, etc. Wujek and Hrnjak (2006) showed that for different orientations and configurations of the sampling cylinder, for a system running on R744 and PAG 46 oil, the measured OCR values were different. But since R744 is not completely miscible in PAG 46 oil in all conditions, it was not clear whether the discrepancies were due to the immiscibility or due to the sampling technique employed.

In the present work, a closer look was taken at the oil sampling techniques involving a horizontal flow-through sampling cylinder and a vertically placed evacuated sampling cylinder with a "dead end" at the top. The compressor speed was varied from 1500 min^{-1} to 2500 min^{-1}. The OCR data obtained from these two techniques were compared with the data from an online oil concentration sensor which was also installed in the setup. The sampling cylinders were made of transparent polyvinyl chloride (PVC) tubing, and this allowed visualization of the flow patterns inside using a high-speed camera. The images of flow into the evacuated sampling cylinder provided interesting information about the OCR data obtained using this method, and some of the factors which may affect the data.

2. EXPERIMENTAL FACILITY

A schematic diagram of the experimental facility is provided in Figure 1. Figure 2 shows images of the different components of the facility currently in use. The experimental setup consists of a vapor compression air-conditioning setup with a compressor, an evaporator, and a condenser inside environmental chambers, and an EEV. The temperatures inside the environmental chambers were maintained at the AHRI A_{Full} condition as prescribed in AHRI standard 210/240 (2017), with the outdoor temperature (condenser air-side temperature) at 95°F (35°C) and the indoor temperature (evaporator air-side temperature) at 80°F (26.7°C). Heaters, blowers, and cooling water circuit are available inside the environmental chambers to ensure that the desired conditions can be achieved at steady-state condition. The refrigerant used for the study was R134a, and the lubricant was PAG 46 oil (this is a miscible combination of oil and refrigerant). The pressure, temperature, mass flow, etc. data are collected and transferred to a data-logger, which then sends the data to a VEE software that provides the real-time values and graphs. The software has a recording feature with an interval of 5 seconds. At steady-state condition, the recorded data are time averaged. Properties of refrigerants and other fluids are calculated using REFPROP 10.0 (2018). Details about the different components of the setup are presented in Table 1.

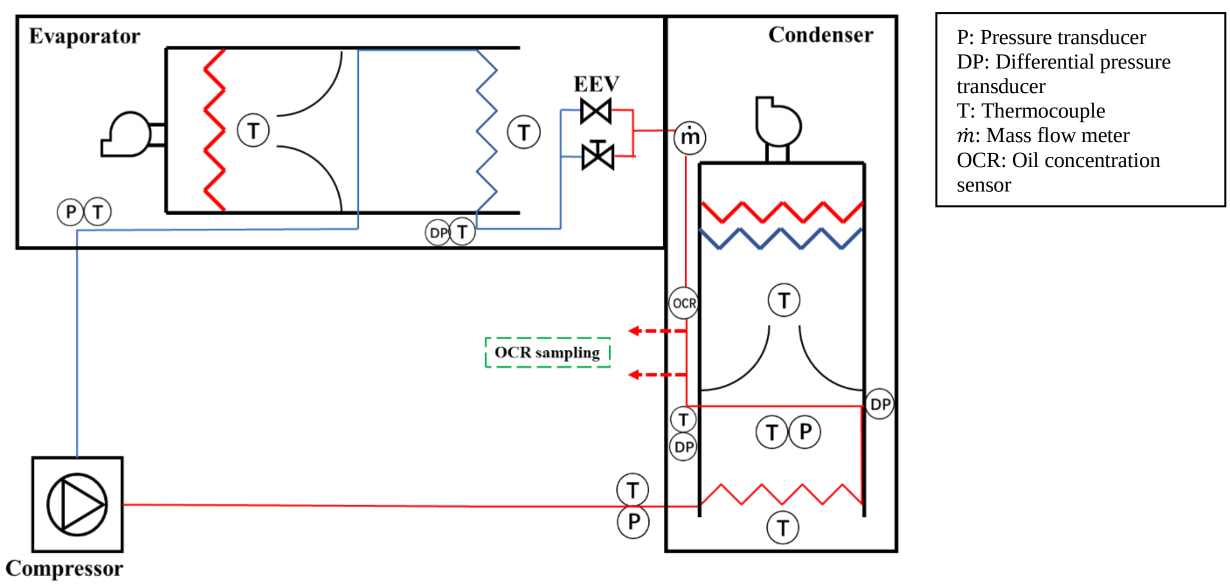

Figure 1: Schematic of experimental facility

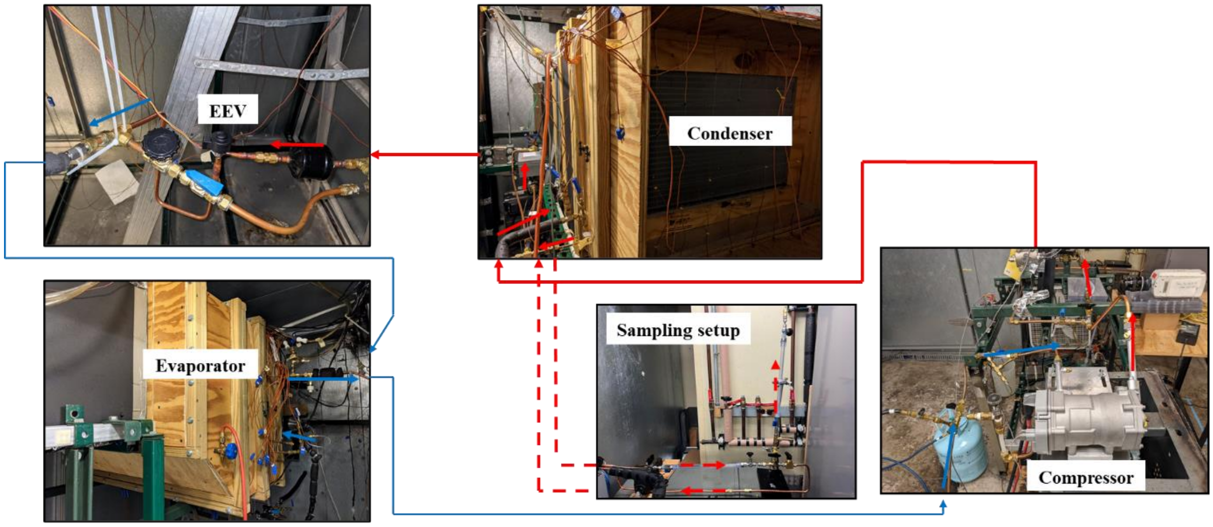

Figure 2: Different components of the experimental facility

Table 1: Details of different equipment

Compressor	**Condenser and evaporator**	**Thermocouples**	**Pressure transducers**	**Mass flow meter**	**Oil concentration sensor**
Variable speed electric scroll	Microchannel type	T-type	Gauge pressure transducers	Coriolis type	Based on speed of sound

The uncertainties of the different sensors used in the experimental facility are provided in Table 2. However, the uncertainties in thermophysical properties are not included in these uncertainties. For the OCR values, uncertainty propagation gave absolute uncertainty in the order of ±0.001. However, there can be many other non-quantifiable sources of uncertainty and so two digits after the decimal point were taken for all the OCR values reported.

Table 2: Uncertainties of different equipment

Instrument	**Thermocouple [°C]**	**Pressure transducer [kPa]**	**Mass flow meter [g/s]**	**Electronic mass balance [g]**	**Wattmeter [kW]**
Uncertainty	±0.2	±3.5	±0.2%	±0.001	±0.5%

3. OCR SAMPLING

3.1 Calculation of OCR

The method of OCR sampling involves taking a sample of oil-refrigerant mixture from the liquid line of the system, and then completely removing all the refrigerant from the sampling cylinder to leave just the oil inside. If the dry mass of the evacuated sampling cylinder is known, the mass of oil in the sample can be calculated, and the OCR will be the ratio of the mass of oil to the total mass of the oil-refrigerant mixture entrapped within the cylinder. The flow-chart for OCR sampling is provided in Figure 3. The OCR in the sample is calculated using Equation (1).

$$OCR = \frac{m_{oil}}{m_{oil} + m_{refrigerant}} = \frac{M_3 - M_1}{M_2 - M_1} \tag{1}$$

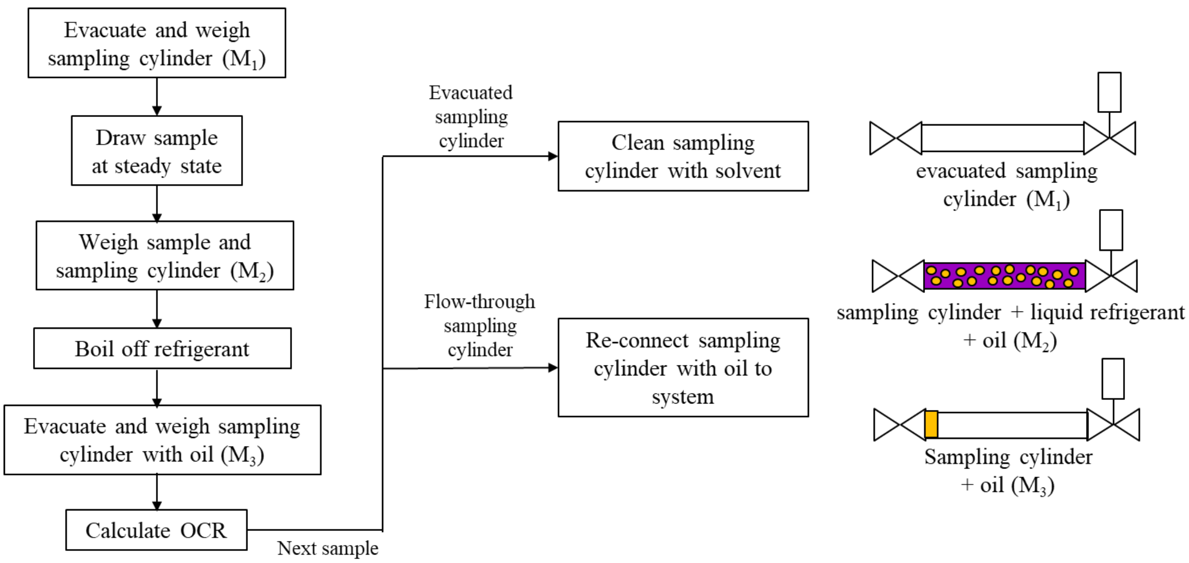

Figure 3: Flow-chart for OCR sampling

3.2 Sampling Configurations Implemented

In the present work, two different configurations of OCR sampling cylinders have been used: the horizontal flow-through type sampling cylinder, and the evacuated vertical sampling cylinder with the dead end at the top. The two configurations as used in the present research (both at the bypass from the liquid line) are shown in Figure 4.

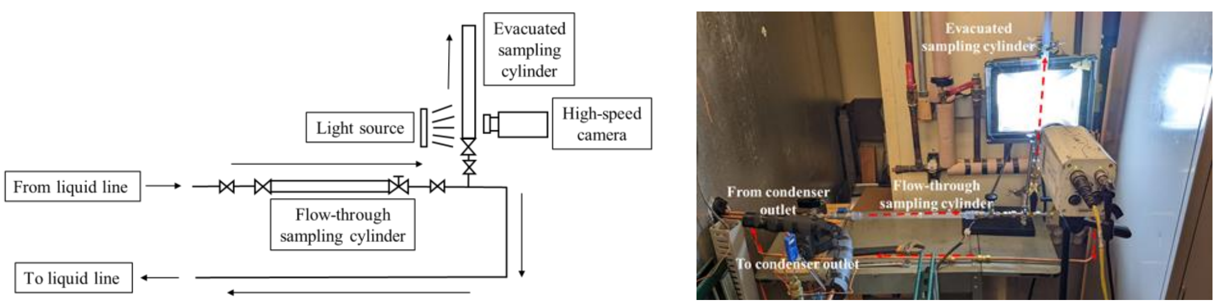

(a) Schematic of OCR sampling setup

(b) Actual OCR sampling setup

Figure 4: OCR sampling setup

For the flow-through case, the oil-refrigerant mixture from the condenser outlet is allowed to flow through the sampling cylinder. Once system steady-state condition is achieved, the valves on the cylinder are closed, and the liquid line flow is made to bypass the sampling cylinder via a three-way valve. But for the evacuated cylinder, a strong vacuum (using 6 a CFM vacuum pump with high vacuum rating) is run through the cylinder, and one end of the cylinder is then connected to the liquid line, while the other end acts as a dead end to the flow. In steady-state, the oil-refrigerant mixture is allowed into the cylinder via valves, and the mixture fills the cylinder. The valves are closed when pressure equalization is realized. Pressure equalization is confirmed when there is no liquid level change in the sampling cylinder, or after five minutes of opening the sampling cylinder valve.

After the OCR has been calculated, the flow-through sampling cylinder is vacuumed strongly. Then it is ready for the next sample, and once it is connected back to the liquid line, the oil is allowed to return to the system. But for the evacuated sampling cylinder, the oil is washed out using a solvent (pure liquid refrigerant R134a was used as solvent since other solvents such as acetone can weaken the sampling cylinders made of PVC). Finally, a strong vacuum is run on it to remove any remaining solvent. Once completely evacuated, the cylinder is ready for the next sample. The removed oil is replenished by returning oil of equal mass at the compressor suction.

4. FLOW VISUALIZATION

For flow visualization at different locations, a high-speed camera (2100 frames/second at a full resolution of 512 x 512 pixels) was used. To relate the flow coming out of the compressor discharge to the measured OCR data, the video of the flow at the discharge tube was taken using the high-speed camera. The flow at the discharge provides qualitative evidence for the obtained OCR results. The discharge tube visualization setup is shown in Figure 5.

One of the goals of the present study was to also observe the flow pattern of the oil-refrigerant mixture going into the evacuated type sampling cylinder, and to find limitations and/or drawbacks of using this method. Again, a high-speed camera was used to take pictures, the setup is shown in Figure 6.

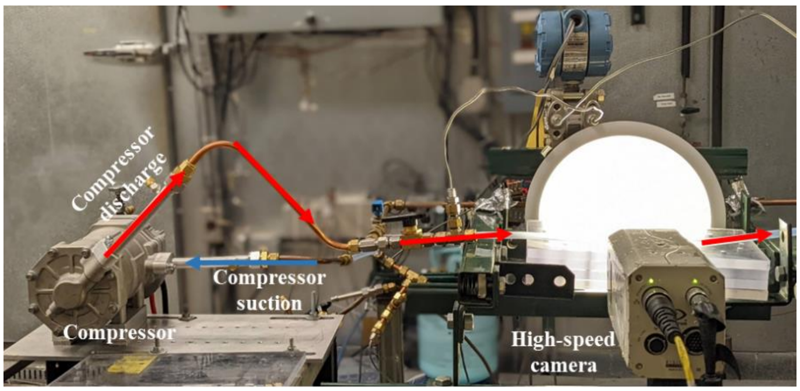

Figure 5: Flow visualization at compressor discharge

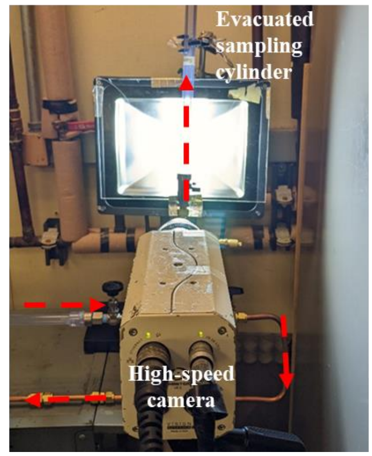

Figure 6: Flow visualization at evacuated sampling cylinder entrance

5. RESULTS

5.1 Comparison of OCR Data

The OCR data were calculated using Equation (1) by the two different sampling techniques, namely, the evacuated sampling cylinder and the flow-through sampling cylinder. The online oil concentration sensor also provided real-time OCR data. All data were taken with the system at steady-state condition, at five different compressor speeds. The compressor speed range available for the electric scroll compressor was 1100 min^{-1} to 2650 min^{-1}, so, for the present work, the OCR was investigated between 1500 min^{-1} to 2500 min^{-1} at 250 min^{-1} intervals. For sampling data, the OCR at each data point was taken to be the average of three separate samples taken, ignoring occasional anomalous values. The real-time data obtained from the online sensor was averaged at steady-state condition. The obtained OCR results are presented in Figure 7.

The OCR results showed an interesting trend: a peak was observed at a compressor speed of 2000 min^{-1} for both the flow-through sampling results, and the online sensor data. The evacuated sampling data showed a peak at a speed of 2250 min^{-1}. Usually, the oil circulation rate increases with compressor speed. As the compressor runs at higher speed, it is expected to also pump out more oil. The flow-through sampling cylider data are thought to be the most reliable for the present study since steady-state samples were taken while the system was running with the use of valves, and sampling cylinder completely filled with liquid oil-refrigerant mixture was obtained.

To gain more insight about the system, and to better understand the obtained OCR results, the high-speed camera images of the flow at the compressor discharge were taken at steady-state. The results of flow visualized at the compressor discharge are discussed in sub-section 5.2.

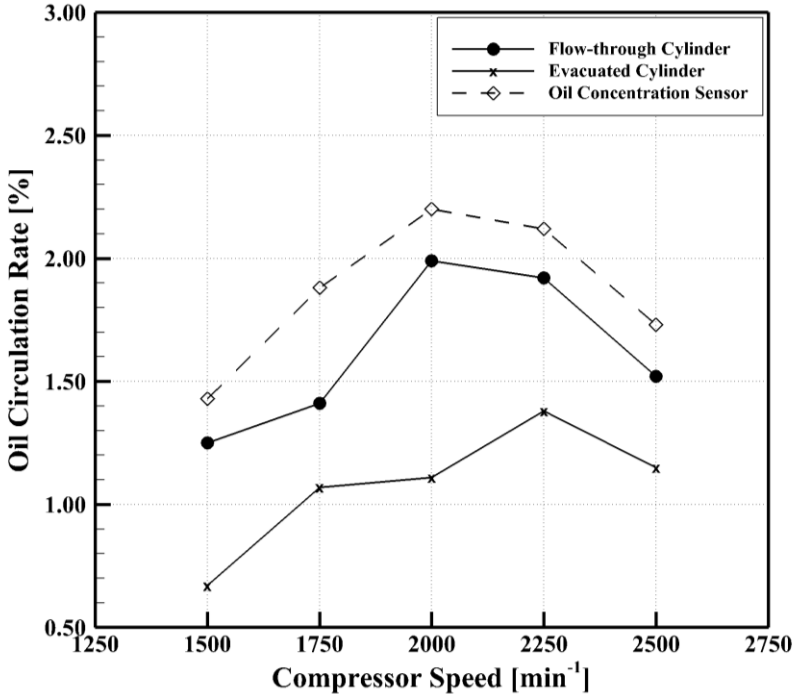

Figure 7: OCR results

5.2 Flow Visualization at Compressor Discharge

Once steady-state condition was achieved at the desired outdoor and indoor conditions, the high-speed camera images of the flow at the compressor discharge were taken, courtesy of transparent perfluoroalkoxy (PFA) tubes downstream of the compressor outlet. The images at speeds of 1500 min^{-1}, 2000 min^{-1} (peak for flow-through and online sensor) and 2500 min^{-1} are provided in Figure 8 (flow from left to right).

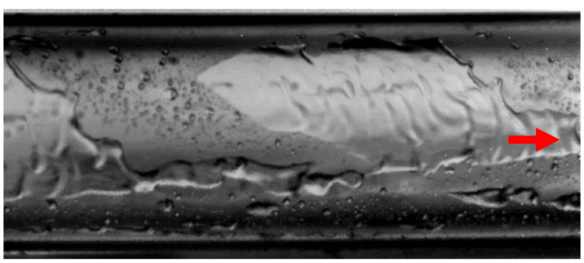

(a) Compressor discharge (1500 min^{-1})

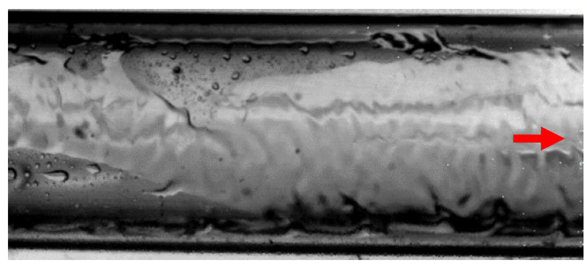

(b) Compressor discharge (2000 min^{-1})

(c) Compressor discharge (2500 min^{-1})

Figure 8: Visualization of flow at compressor discharge

At 1500 min^{-1}, the flow consisted of small droplets of oil, some of which merged to form oil streams. There were some occasional films, but most were not stable or continuous, and broke down. Usually, film oil flow at the discharge indicates higher OCR, while droplets and streams usually characterize less oil being pumped out of the compressor. So, the low OCR values agree with the flow at the discharge. For 2000 min^{-1}, which showed a peak for the flow-through and online sensor cases, a more stable film can be observed, and fewer droplets can be seen. However, the film for this case also wasn't very stable, and broke down at some locations. Finally, for the 2500 min^{-1} case, there were no films, only small droplets, and some droplets coalesced into larger ones, sometimes into oil streams. Since the OCR values were small, a continuous oil film wasn't seen at the discharge. These results agree with the trend in OCR values that can be seen in Figure 7. Even though the flow at the compressor discharge supports the trend in OCR, it doesn't necessarily explain the trend. With insufficient knowledge about the internal structure of the compressor, it is difficult to come to a conclusion about the trend.

5.3 Flow Visualization at Evacuated Sampling Cylinder Entrance

While conducting experiments using the evacuated sampling cylinder, it was observed that the opening speed of the valve (mini ball valve, K_v = 4.5 m^3/h when fully open) on the sampling cylinder affected the flow going into it. To take a closer look, the high-speed camera was used to take images of the flow going into the evacuated sampling cylinder for fast (0.5 second) and slow (3 seconds) valve opening speeds at compressor speed of 2250 min^{-1} (peak for evacuated cylinder). The images are provided in Figures 9 and 10.

For the fast valve opening case, from Figure 9, in (a) and (b), when the valve is first opened, mostly vapor refrigerant begins to enter the sampling cylinder and this is because the opening is small and refrigerant flashing occurs. But soon after, in (c) and (d), tiny liquid droplets attach to the walls (left and right side of image), and these droplets are expected to consist of oil-rich liquid mixture, but it is hard to differentiate the two. As the valve opens more in (e), vapor and liquid start to enter the cylinder, and begin to fill it up. The vapor characterized by the shadows, and the liquid seen as droplets and slugs mostly move up the sampling cylinder due to the large pressure difference, finally going from a foamy flow in (f) to (h), to finally transparent region of liquid oil-refrigerant mixture as seen in (i). The OCR obtained for the fast valve opening case was 1.45% (average of 3 samples).

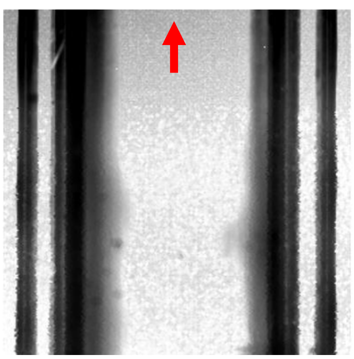

(a) t = 0.000 s

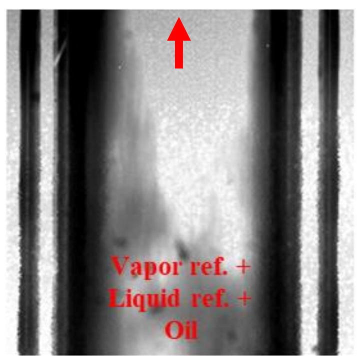

(b) t = 0.005 s

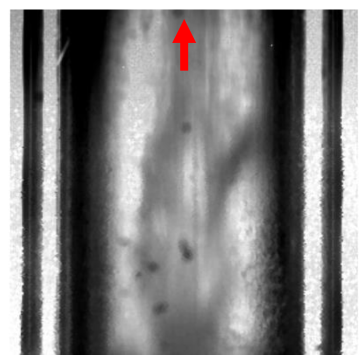

(c) t = 0.008 s

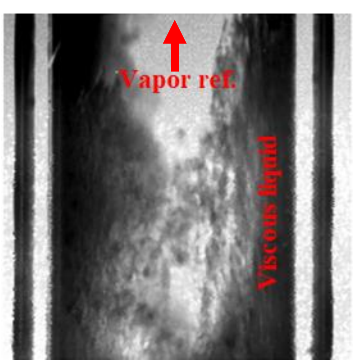

(d) t = 0.014 s

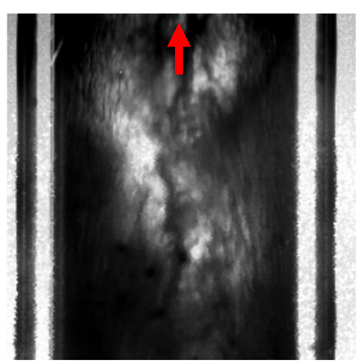

(e) t = 0.027 s

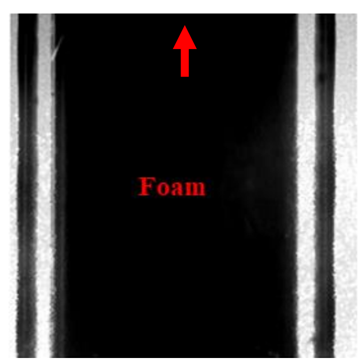

(f) t = 0.083 s

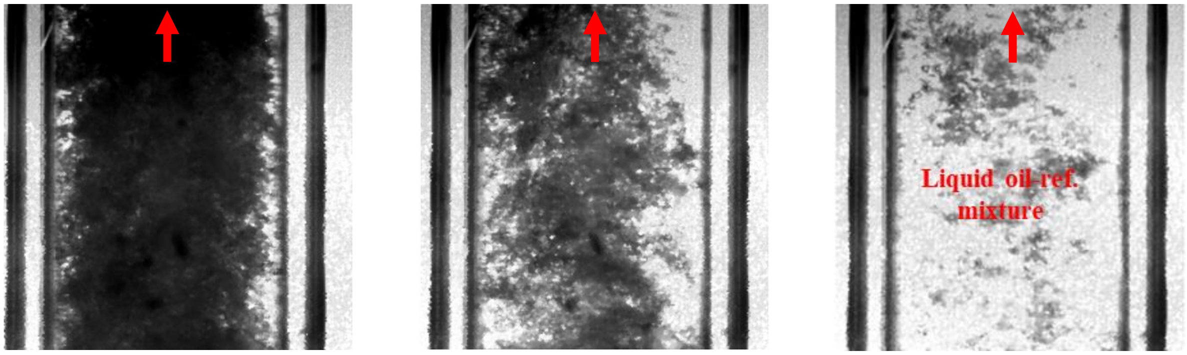

(g) *t* = 0.310 s (h) *t* = 0.351 s (i) *t* = 0.368 s

Figure 9: Flow entering evacuated cylinder for fast valve opening

When the valve on the evacuated sampling cylinder was opened slowly, the flow patterns observed showed differences from the fast-opening case. As seen in Figure 10, for slow valve opening, initially there is vapor going into the cylinder as in (a), but as the valve opens more, a layer of liquid can be seen on the cylinder walls (left and right side of images) in (b), and this indicates an oil-rich region with refrigerant dissolved in it. As the valve opens more, vapor refrigerant characterized by shadows moves up into the cylinder, but the liquid is seen to circle back downwards instead of moving up to fill the cylinder as seen in (c) to (e). When the opening gets larger, a foaming region in observed in (f) to (h), which then transitions to a transparent region indicating liquid oil-refrigerant mixture which fills up the cylinder due to the large pressure difference as seen in (i). The OCR measured for the slow valve opening case was 1.32% (average of 3 samples), which is lower than the fast-opening case even though the experimental conditions and compressor speeds were the same.

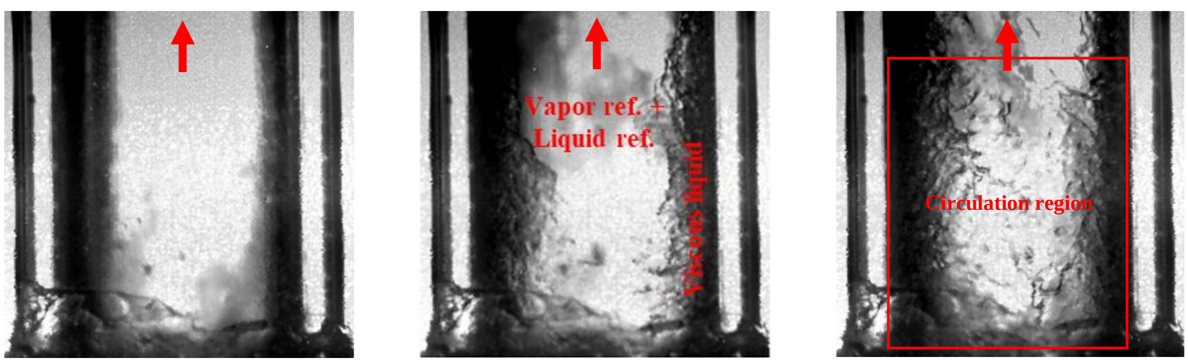

(a) *t* = 0.000 s (b) *t* = 0.017s (c) *t* = 0.034 s

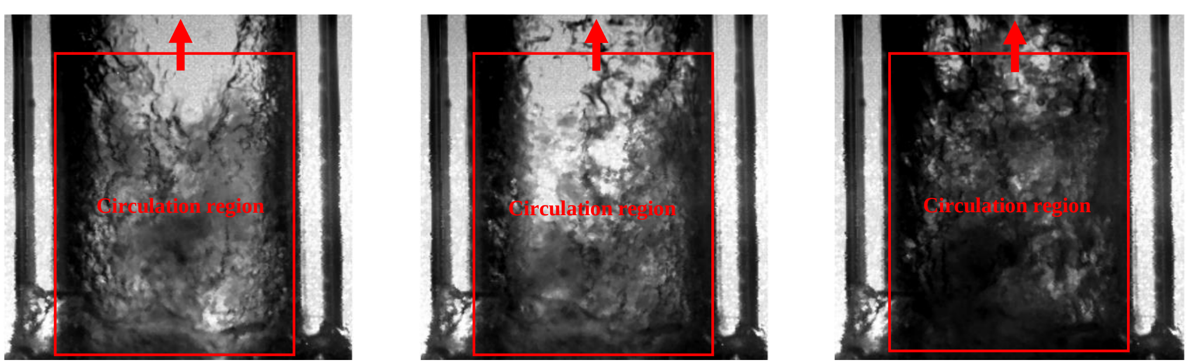

(d) *t* = 0.067 s (e) *t* = 0.106 s (f) *t* = 0.162 s

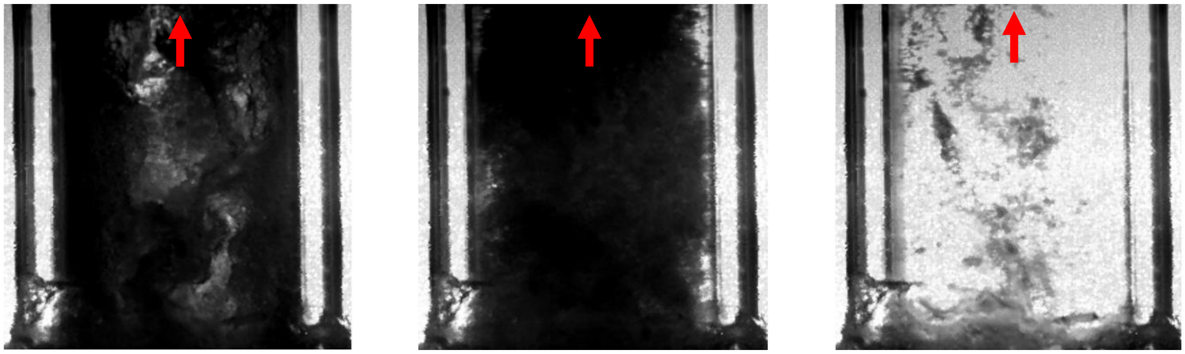

(g) t = 0.250 s (h) t = 0.587 s (i) t = 0.639 s

Figure 9: Flow entering evacuated cylinder for slow valve opening

The results of the slow and fast valve opening cases were quite interesting since they indicated discrepancies due to how fast the sampling cylinder valves were being opened. It is suspected that when the valve is opened slowly, some of the oil flows back down into the fittings rather than moving up to fill the tube. As a result, the total oil content in the similarly sized sample is lower for slow opening. The ASHRAE standard 41.4 (2015) does not indicate how the sampling cylinder valves should be opened for accurate OCR measurement.

Alongside valve opening speed, other factors could also affect the OCR data measured using the evacuated type sampling cylinder. Some potential factors include the sampling cylinder orientation as investigated by Haider *et al*. (2022), shape of the sampling cylinder, oil-refrigerant combination used, time of refrigerant evacuation after sampling, etc.

6. CONCLUSIONS

Knowledge of oil circulation rate and its accurate measurement are crucial for proper system optimization. But most OCR measurement techniques rely on calibration using OCR sampling. The ASHRAE standard describes the method for OCR sampling, but it has some limitations and is sometimes open to interpretation as evidenced by the present work. This paper presents the OCR results from a flow-through cylinder and an evacuated cylinder method of OCR sampling. An online oil concentration sensor was used to validate the trend in the data. Discrepancies were observed between flow-through and evacuated styles of sampling, with the flow-through data being consistently higher than the evacuated cylinder data. The OCR data from all three measurements showed a peak. The high-speed camera images revealed a more stable oil film at the peak than at speeds on either side of the peak which mostly included oil droplets and streams, thus supporting the OCR results. However, the exact explanation for the OCR results was not conclusively found due to insufficient knowledge about the interior of the compressor sample, and how well it worked with the system. The evacuated sampling cylinder data showed difference due to speed of valve opening, which was suspected to occur due to oil-rich mixture flowing back out of the cylinder into the fittings below. This was, however, just one of the several factors which can affect the OCR data obtained using the method described by the ASHRAE standard. The orientation of the sampling cylinder, shape of the cylinder, oil-refrigerant combination used, time of refrigerant evacuation after sampling and many other factors could play a role in affecting the data, and these pave the path for future investigation and research.

NOMENCLATURE

T	temperature	(°C)
P	pressure	(kPa)
DP	differential pressure	(kPa)
M, m	measured or calculated mass	(g)
t	time	(s)
$\dot{m}$	mass flow rate	(g/s)

Q	power/capacity	(kW)
OCR	oil circulation rate	(%)
K_v	flow coefficient	(m^3/h)

Subscript

oil	oil in system
refrigerant	refrigerant in system

REFERENCES

AHRI, A. (2017). 210/240-Standard for Performance Rating of Unitary Air Conditioning and Air-Source Heat Pump Equipment. *Air-Conditioning, Heating, and Refrigeration Institute*.

Haider, S. A., Wang, X., & Elbel, S. (2022). Effects of Orientation and Valve Opening Speed on Oil Circulation Rate Measurements Using an Evacuated Type Sampling Cylinder. *Proceedings of the International Refrigeration and Air Conditioning Conference*, Paper 2214, West Lafayette, IN, USA.

Liu, X., & Hrnjak, P. (2016). Oil effects on performance of automobile A/C system. *Proceedings of the International Refrigeration and Air Conditioning Conference*, Paper 1672, West Lafayette, IN, USA

Radermacher, R., Cremaschi, L., & Schwentker, R. A. (2006). Modeling of oil retention in the suction line and evaporator of air-conditioning systems. *HVAC&R Research*, *12(1),* 35-56.

REFPROP, N. (2018). Reference fluid thermodynamic and transport properties. *NIST Standard Reference Database, 23*.

Shen, B., & Groll, E. A. (2005). A critical review of the influence of lubricants on the heat transfer and pressure drop of refrigerants, Part 1: Lubricant influence on pool and flow boiling. *HVAC&R Research*, *11(3),* 341-359.

Standard, ASHRAE Standard 41.4-2015, 2015. *Standard Method for Measurement of Proportion of Lubricant of Liquid Refrigerant. ASHRAE*, Atlanta, GA, USA.

Wujek, S. S., & Hrnjak, P. (2006). Effects of Oil on a Transcritical Carbon Dioxide Air Conditioning Systems–some experiences. *Proceedings of the International Refrigeration and Air Conditioning Conference*, Paper 164, West Lafayette, IN, USA

Xu, J., & Hrnjak, P. (2017). Quantification of flow and retention of oil in compressor discharge pipe. *International journal of refrigeration, 80,* 252-263.

Youbi-Idrissi, M., & Bonjour, J. (2008). The effect of oil in refrigeration: Current research issues and critical review of thermodynamic aspects. *International Journal of Refrigeration, 31(2),* 165-179.

ACKNOWLEDGEMENT

The authors would like to thank the member companies of the Air Conditioning and Refrigeration Center at the University of Illinois at Urbana-Champaign for their funding to support this project, Bergstrom Inc. for providing the compressor sample, Sanhua for providing EEV samples, and Creative Thermal Solutions, Inc. for technical support. The authors would also like to thank Sugun Tej Inampudi for his help and for proofreading our work, and Tokitaka Yoshida and Jun Li for their invaluable advice on different pieces of HVAC&R equipment.